Journal of Optoelectronics and Advanced Materials Vol. 7, No. 2, April 2005, p. 1079 - 1090

DETERMINATION OF THE DIFFUSION COEFFICIENTS FOR TERNARY SYSTEMS BY GOSTING DIFFUSIOMETER. APPARATUS AND METHOD

D. Buzatu*, E. Petrescu, C. Popa, F. D. Buzatu[a]

Physics Department, "Politehnica" University, Bucharest, 77206, Romania
[a]Department of Theoretical Physics, National Institute for Physics and Nuclear Engineering, Bucharest-Magurele, 76900, Romania

In this paper we describe the Gosting interferometric optical diffusiometer operating in Rayleigh mode and the theoretical approach about diffusion applied to ternary lysozyme-Na_2SO_4-water system. Gosting diffusiometer is a unique instrument which was designed and constructed for diffusion measurements in multicomponent liquid systems, with particular interest in aqueous protein system, and located in Texas Christian University, Department of Chemistry. The experimental analysis work for ternary lysozyme-Na_2SO_4-water system at pH = 4.5 and T = 25 ^oC, including the baseline scans, boundary sharpening, fractional part of fringe scans, diffusion scans and data analysis are also presented.

(Received December 7, 2004; accepted March 23, 2005)

Keywords: Gosting diffusiometer, Rayleigh interferometric method, Data analysis for lysozyme-Na_2SO_4-water

1. Introduction

Protein diffusion plays an important role in many biochemical processes. In particular, diffusion of protein is important in medicine, laboratory and manufacturing applications. Examples include centrifugation, dialysis and crystallization. Effective modeling, prediction and design of these processes require accurate descriptions of protein transport. Protein systems are invariably multicomponent in nature, due to the buffers, added salts or other macromolecules typically present.

The complete description of an *n*-solute system requires an $n \times n$ matrix of diffusion coefficients relating the flux of each solute component to the gradients of all solute components [1]. Since experience with other multicomponent systems shows that cross-terms in the diffusion coefficient matrix are often significant, the validity of the common assumption of pseudo-binary protein diffusion can only be assessed by measuring the full set of n^2 diffusion coefficients [1,2].

A very important scientific application in which protein diffusion is critical is the growth of large crystals with low defect densities, a critical step in the use of X-ray crystallography to determine protein structure. There is a large body of experimental and theoretical works about the central role of diffusion in protein crystal growth phenomena.

First, diffusion determines the concentration profiles within a protein-depleted zone immediately adjacent to the growing crystal [3,4]. Second, diffusion of precipitant and impurities is critical to impurity and precipitant incorporation into or rejection from the growing crystal [5]. Third, diffusion is important in establishing the concentration gradients for the buoyancy-driven convective flow that can arise in protein crystal growth experiments under normal gravity conditions [6].

Finally, the diffusion is the dominant transport mechanism [7] when the protein crystal growth is conducted under microgravity conditions. The difference between microgravity and normal gravity is the magnitude of the buoyancy forces. Commonly, this difference is assigned to some consequences of the reduction of buoyancy driven convection in the microgravity conditions. Due to convection, the protein concentration in the bulk solution is more uniform [7] and the probability for nucleation of parasitic crystals is strongly reduced.

* Corresponding author: danielle_buzatu@yahoo.com

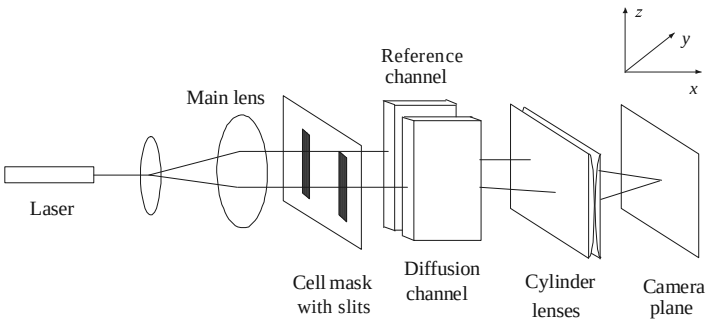

Fig. 1. Scheme of the optical apparatus working in Rayleigh configuration.

2. Theoretical approach

Rayleigh optical interferometric method is the most precise and accurate method for the determination of the mutual diffusion coefficients. This method permits the determination of one-dimensional refractive index profile of a liquid system contained in a cell with rectangular geometry [8]. This refractive index profile, under certain initial and boundary conditions, can be quantitatively analyzed giving quantitative information on the diffusion process [9].

In the Rayleigh configuration, the light is generated by a LASER source containing a slit of adjustable width which is illuminated by monochromatic light (Fig. 1). The slit can be rotated to be either horizontal or vertical for use with the Gouy fringe or Rayleigh integral fringe methods, respectively. The light is rendered convergent by a main spherical lens that focuses slit image to a "camera" plane. Then two coherent beams are generated by two vertical slits positioned between the convergent lens and the measuring cell. One beam goes through the diffusion channel and one through the reference channel of the experimental cell. The interference pattern is then collected on the "camera" plane. The distance between the fringes is determined by the separation of the two slits, while the absolute shift of the fringes is proportional to the difference in the optical path between the two beams. If the refractive index is uniform in the diffusion channel along the Z direction, the value of the Y position of the maxima at the camera plane will be invariant with Z. Thus, straight interference lines are produced as in the Young's interference experiment.

If the refractive index inside of the diffusion channel changes along the Z direction, the rays are deflected by the gradient of refractive index and a system of cylindrical lenses is needed to reverse effectively the deflection and to focus the cell onto the "camera" plane. Fig. 2 gives a scheme of the Rayleigh interferometric pattern of the fringes profile proportional to the refractive index profile.

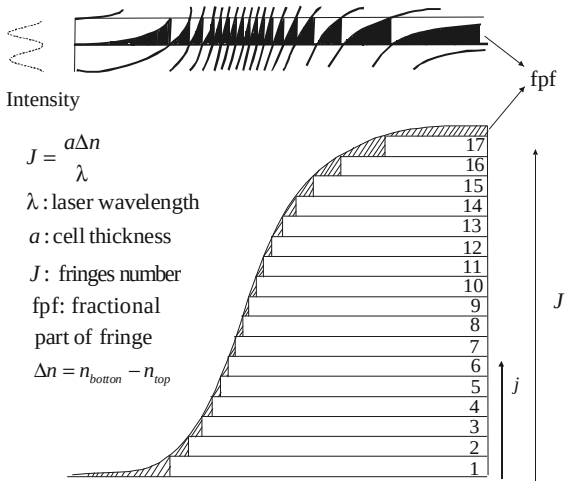

Fig. 2. Scheme of the Rayleigh interferometric pattern and refractive index profile; the solid lines correspond to maxima positions.

In the case of diffusion between solutions of two different concentrations c_i^{top} and c_i^{bottom} of the same solute, i, it has been found that the measured diffusion coefficient is associated with a system having the solute average concentration equal to $\bar{c}_i = \left(c_i^{top} + c_i^{bottom}\right)/2$, where the concentration dependence of the diffusion coefficient is relatively small. Gosting, Fujita and Creeth [10-14] have given the largest contribution for developing the equations that provide the extraction of the diffusion quantities by the refractive index profile analysis.

The overall fringe displacement between the two extreme parts of the pattern, reported as a multiple of the distance between two parallel adjacent fringes, is called the total number of fringes J. This quantity, not necessary an integer, is related to the refractive index difference, Δn, between the two solutions across the initial boundary, by the relation:

$$J = \frac{a}{\lambda}\Delta n \tag{1}$$

where a is the geometric path inside the cell (diffusion channel thickness) and λ is the LASER wavelength. The refractive index of j fringe, n_j, is related to fringe number j, and to the total number of fringes, J, by the function $f(j)$:

$$f(j) = \frac{2j - J}{J} = \frac{2\left(n_j - \bar{n}\right)}{\Delta n} \tag{2}$$

where j is a continuous variable with values ranging between 0 and J, $\bar{n} = \left(n_{bottom} + n_{top}\right)/2$, and $\Delta n = n_{bottom} - n_{top}$ is the total difference of refractive index across the starting boundary. This function $f(j)$ has the property of being equal to zero at the center of pattern and equal to respectively -1 and $+1$ at the two boundaries [9].

In the case of ideal systems, both the diffusion coefficient, D, and the differential refractive increment, $R = \frac{\partial n}{\partial c}$, are independent of concentration, and the refractive index is a linear function of the solute concentration.

For a ternary system, like our ternary lysozyme-Na_2SO_4-water system, characterized by mean concentrations of the two solutes

$$\bar{c}_1 = \frac{c_1^{top} + c_1^{bottom}}{2} \quad ; \quad \bar{c}_2 = \frac{c_2^{top} + c_2^{bottom}}{2} \tag{3}$$

and differences

$$\Delta c_1 = c_1^{bottom} - c_1^{top} \quad ; \quad \Delta c_2 = c_2^{bottom} - c_2^{top} \tag{4}$$

we assume that both the diffusion matrix

$$\left|D_{ij}\right| = \begin{vmatrix} D_{11} & D_{12} \\ D_{21} & D_{22} \end{vmatrix} \tag{5}$$

and refractive index derivatives

$$R_1 = \left.\frac{\partial n}{\partial c_1}\right|_{T,p,c_2=\bar{c}_2} \quad ; \quad R_2 = \left.\frac{\partial n}{\partial c_2}\right|_{T,p,c_1=\bar{c}_1} \tag{6}$$

are concentration independent. Also we assume a linear dependence of refractive index on concentrations c_1 and c_2:

$$n(c_1, c_2) = \bar{n} + R_1(c_1 - \bar{c}_1) + R_2(c_2 - \bar{c}_2) \tag{7}$$

The Fick's first and second law, for interacting flows in ternary systems become:

$$j_1 = -D_{11}\frac{\partial c_1}{\partial x} - D_{12}\frac{\partial c_2}{\partial x} \quad ; \quad j_2 = -D_{21}\frac{\partial c_1}{\partial x} - D_{22}\frac{\partial c_2}{\partial x} \tag{8}$$

and

$$\frac{\partial c_1}{\partial t} = D_{11}\frac{\partial^2 c_1}{\partial x^2} + D_{12}\frac{\partial^2 c_2}{\partial x^2} \quad ; \quad \frac{\partial c_2}{\partial t} = D_{21}\frac{\partial^2 c_1}{\partial x^2} + D_{22}\frac{\partial^2 c_2}{\partial x^2} \tag{9}$$

where D_{11} and D_{22} are the main diffusion coefficients and D_{12} and D_{21} are the cross-term diffusion coefficients.

Under the initial conditions:

$$x < 0, \quad t = 0, \quad c_1 = c_1^{bottom} \quad ; \quad c_2 = c_2^{bottom} \tag{10}$$

$$x > 0, \quad t = 0, \quad c_1 = c_1^{top} \quad ; \quad c_2 = c_2^{top} \tag{11}$$

and the free diffusion boundary conditions:

$$x \to -\infty, \quad c_1 \to c_1^{bottom}, \quad c_2 \to c_2^{bottom} \tag{12}$$

$$x \to \infty, \quad c_1 \to c_1^{top}, \quad c_2 \to c_2^{top} \tag{13}$$

we obtain the solutions of the differential equations (9) [11] as a sum of two probability integrals $\Phi(z)$:

$$c_1 = \bar{c}_1 + K_1^+\Phi(z_+) + K_1^-\Phi(z_-) \quad ; \quad c_2 = \bar{c}_2 + K_2^+\Phi(z_+) + K_2^-\Phi(z_-) \tag{14}$$

with

$$z_+ = \sqrt{\sigma_+}\, y \ , \quad z_- = \sqrt{\sigma_-}\, y \ , \quad y = \frac{x}{2\sqrt{t}} \tag{15}$$

where σ_+ and σ_- are the reciprocal of the eigenvalues of the diffusion coefficients matrix.

The subscripts "+" and "-" of σ denote the positive and negative values of the square-root term in the expression:

$$\sigma_+ = \frac{1}{2}\left[\frac{D_{22} + D_{11} + \sqrt{\theta}}{D_{11}D_{22} - D_{12}D_{21}}\right] \quad ; \quad \sigma_- = \frac{1}{2}\left[\frac{D_{22} + D_{11} - \sqrt{\theta}}{D_{11}D_{22} - D_{12}D_{21}}\right] \tag{16}$$

where:

$$\theta = (D_{22} - D_{11})^2 + 4D_{12}D_{21} \tag{17}$$

The coefficients of the probability integrals K_1^+, K_1^-, K_2^+ and K_2^- are given by:

$$K_1^+ = \frac{(D_{22} - D_{11} + \sqrt{\theta})\Delta c_1 - 2D_{12}\Delta c_2}{4\sqrt{\theta}} \quad ; \quad K_1^- = \frac{(D_{22} - D_{11} - \sqrt{\theta})\Delta c_1 - 2D_{12}\Delta c_2}{-4\sqrt{\theta}} \tag{18}$$

$$K_2^+ = \frac{(D_{11} - D_{22} + \sqrt{\theta})\Delta c_2 - 2D_{21}\Delta c_1}{4\sqrt{\theta}} \quad ; \quad K_2^- = \frac{(D_{11} - D_{22} - \sqrt{\theta})\Delta c_2 - 2D_{21}\Delta c_1}{-4\sqrt{\theta}} \tag{19}$$

It may be seen from relation (14) that interaction of solute flows does not produce skewness of the concentration gradient curves, provided that the diffusion coefficients are independent of concentrations.

The refractive index distribution for free diffusion in a three-component system with interacting flows is obtained by substituting the solution (14) for c_1 and c_2 into equation (7):

$$n = n(\bar{c}_1, \bar{c}_2) + \frac{\Delta n}{2}\left[\Gamma_+ \Phi\left(\sqrt{\sigma_+}\, y\right) + \Gamma_- \Phi\left(\sqrt{\sigma_-}\, y\right)\right] \tag{20}$$

where

$$\Gamma_+ = \frac{2}{\Delta n}\left(R_1 K_1^+ + R_2 K_2^+\right) \quad ; \quad \Gamma_- = \frac{2}{\Delta n}\left(R_1 K_1^- + R_2 K_2^-\right) \quad ; \quad \Gamma_+ + \Gamma_- = 1 \tag{21}$$

Taking into account the eqs. (3, 4, 7) we could express the total refractive index change across the initial boundary as follows:

$$\Delta n = R_1 \Delta c_1 + R_2 \Delta c_2 \tag{22}$$

According to the relations (2) and (20), the fringe number function could be expressed by the following equation:

$$f(j) = \Gamma_+ \Phi\left(\sqrt{\sigma_+}\, y\right) + \Gamma_- \Phi\left(\sqrt{\sigma_-}\, y\right) \tag{23}$$

If we define the refractive fraction,

$$\alpha_1 = \frac{R_1 \Delta c_1}{\Delta n}; \qquad \alpha_2 = \frac{R_2 \Delta c_2}{\Delta n}; \qquad \alpha_1 + \alpha_2 = 1 \tag{24}$$

from relations (18-19) and (21) we obtain the following linear relation:

$$\Gamma_+ = a + b\alpha_1 \tag{25}$$

where a and b are two constants. If we insert the relation (25) into expression (23) and take into account the rel.(21), we obtain the following expression for fringe number function:

$$f(j) = (a + b\alpha_1)\Phi\left(\sqrt{\sigma_+}\, y\right) + (1 - a - b\alpha_1)\Phi\left(\sqrt{\sigma_-}\, y\right) \tag{26}$$

The above equation is sufficient for determination of the D_{ij}, by least-squares procedures.

Least-squares applied to $f(j)$ with respect to the variables (y,α_1) yields the values for the quantities (σ_+,σ_-,a,b). The ternary diffusion coefficients can be then determined by the following set of equations [15]:

$$D_{11}=\frac{(a+b)(1-a)\sigma_- - a(1-a-b)\sigma_+}{b\sigma_+\sigma_-}\ ;\ D_{12}=-\frac{R_2}{R_1}\frac{(\sigma_+-\sigma_-)a(1-a)}{b\sigma_+\sigma_-} \quad (27)$$

$$D_{21}=-\frac{R_1}{R_2}\frac{(\sigma_+-\sigma_-)(a+b)(1-a-b)}{b\sigma_+\sigma_-}\ ;\ D_{22}=\frac{(a+b)(1-a)\sigma_+ - a(1-a-b)\sigma_-}{b\sigma_+\sigma_-} \quad (28)$$

3. Experimental section

All the experimental work, the preparation of the solutions and the measurement of diffusion coefficients, were performed in Texas Christian University, Department of Chemistry.

All solutions were prepared by mass with appropriate buoyancy corrections. All weighings were performed with a Mettler Toledo AT400 electrobalance. Since the received lysozyme powder was very hygroscopic, all manipulations in which water absorption might be critical were performed in a dry glove box.

The pH measurements were made using a Corning model 130 pH meter with an Orion model 8102 combination ROSS pH electrode. The meter was calibrated with standard pH 7 and pH 4 buffers and checked against a pH 5 standard buffer.

All density measurements were made with a Mettler-Paar DMA40 density meter, with an RS-232 output to an Apple Π+. By output time averaging, a precision of 0.00001g/cm or better could be achieved. The temperature of the vibrating tube in the density meter was controlled with water from a large well-regulated water bath whose temperature was $25.00\pm 0.01\ ^oC$.

In order to determine the diffusion coefficients for ternary solution Lysozyme-Na_2SO_4 - water we used the Gosting diffusiometer located in Texas Christian University, USA were we made all the experiments. This Gosting diffusiometer is a unique instrument with a very good quality for optical and mechanical components (Fig. 3) [16].

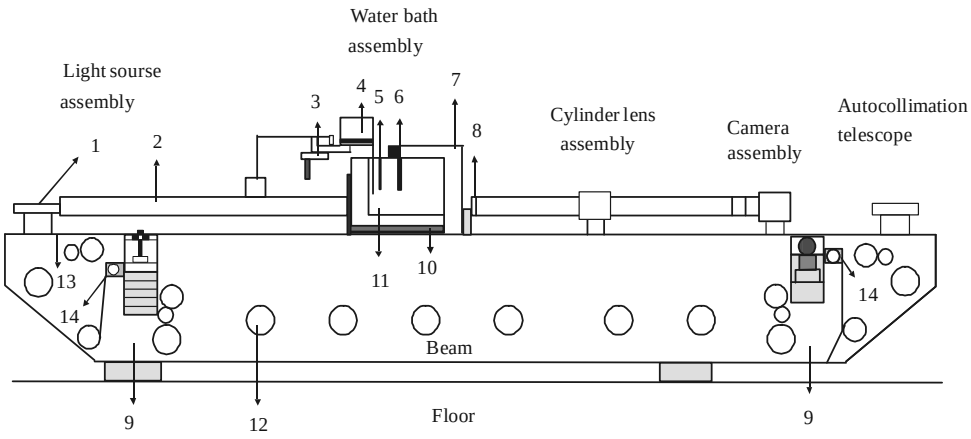

Fig. 3. Schematic drawing of the diffusiometer.1. Slit of light source; 2. tube to minimize air currents in the light path; 3. stirring motor mount; 4. stirring motor; 5. sensor of temperature control; 6. heater; 7. cell frame support; 8. special window rider; 9. beam support; 10. water bath support; 11. water bath; 12. access hole to reach the inside of the beam; 13. ways; 14. leveling collar to check any change in the position of the beam relative to that of beam support; 15. digital optical scanner.

The components of this optical system and the diffusion cell holder are all rigidly supported

on an 8.84 m long steel beam and 5000 kg optical bench mass. It is found that relative positions of optical components remain fixed within a few μm from one end of the bench to the other during an experiment. Vibration isolation is provided by these rubber feet and by the separate mounting of the water bath and stirrer assembly [16].

Gosting diffusiometer has two optical modes of operation: a Gouy interferometric mode which is a one dimensional interferometric pattern [9] and a Rayleigh interferometric mode, which produces at the camera position a record of the vertical refractive index distribution in the cell and this is the two dimensional interferometric pattern.

The light source is a 0.5 mW, 543.4 nm (in air) Uniphase He-Ne LASER.

The main lens is installed in a lens mount on the source slit side of the water bath so that the diffusion cell is in the converging light between the lens and the camera. The lens is a two element air-spaced achromat corrected for the mercury green and blue lines and mounted in a black anodized aluminum lens holder. The focal length was found to be 145.16 ± 0.03 cm.

The cylinder lens consists of two plane-convex lenses, each 7.5 cm square and 1.3 cm thick at its thickest part, made of astronomical objective quality borosilicate crown glass; it was specified that the lens surfaces be accurate within 1/2 wavelength and that the focal length of the pair be 68.0 cm for mercury green light.

A cell holder is used to locate the cell in the bath. The cell holder has also the function of supporting a mask located between the cell and the light source. For the Rayleigh method the mask consists of a double window allowing the beam to split in two parts, one going through the diffusion channel and the other passing directly through the water bath (reference channel).

The cell is glass Tiselius type previously designed for electrophoresis experiments. The cell is composed (Fig. 4) of three pieces put in contact by very smooth plane surfaces. Grease is used to seal the plates and lubricate their sliding relative to each other. The shift of the plates allows the solutions, filled in all three parts, to be either in contact or isolated from each other. The path length of the cell (model C-1235-H11) employed in the measurements is $a = 2.5057$ cm.

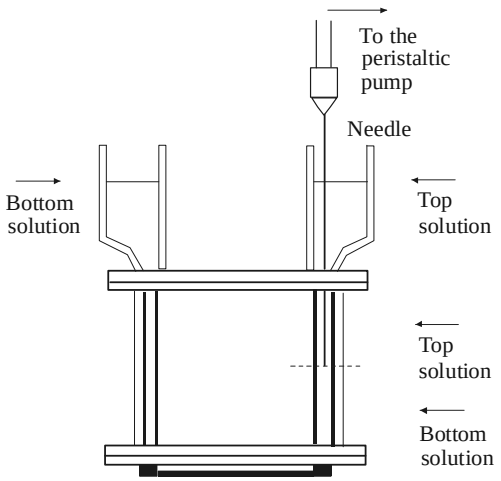

Fig. 4. Tiselius cell; boundary sharpening.

A vertical linear photodiode was used to record the data from Rayleigh interference pattern (6 cm long, 6000 pixel (10X10 μm pixels) linear photodiode array model IL-C8-6000-64 with high light sensitivity that moves horizontally through the pattern.

All programming of scanner control and data analysis were done in *Borland C*$^{++}$ *for DOS*. At the camera plane of the Gosting diffusiometer, the Rayleigh pattern is over 6 cm long (vertically) and 2-3 mm wide, with a fringe separation (horizontally) of roughly 260 μm within the pattern. The diode array is mounted symmetrically on a rotating disk on a mounting plate. The mounting plate is attached to a Grant indicator which could be moved horizontally (Y direction) with a stepping motor, and the relative horizontal position can be measured with an optical encoder. By moving the

array horizontally through a vertical Rayleigh fringe pattern, while recording intensities in the vertical dimension with the diode array, a two dimensional profile of a Rayleigh pattern can be recorded.

The computer used for our purpose was a Pentium III, 500 MHz, IBM compatible PC. The interface board was a standard data acquisition plug-in board PC-30DS/4.

The experimental procedure can be divided in five parts [17,18]: baseline scans, boundary sharpening, fractional part of fringe (fpf) scans, diffusion scans and data analysis.

The *baseline patterns* are scanned using the vertical photodiode and fringe positions are recorded. If the optical components were of perfect quality, these patterns would show straight vertical fringes. However, because of imperfections in these components (including the diffusion cell) these fringes are not perfectly straight, and deviations up to 20 μm are registered along the Y direction. To correct for this deviation when evaluating the diffusion patterns, it is necessary to know the Y shift of the baseline fringes for each pixel of the photodiode array. Baseline patterns are scanned by moving the array in 10 μm increments 53 times to give a scan of 54 positions and 530 μm travel. Intensity data are recorded at each of the 54 positions. Since the vertical fringes are typically separated by about 260 μm, this gives a horizontal intensity profile from each pixel that includes the minima corresponding to the two adjacent "dark fringes" beyond the starting position.

The minima positions were estimated by quadratic fitting on seven intensity points about of each of the two minima. The positions of two fringe minima obtained for each pixel are averaged to give a baseline datum for that pixel for that scan. This datum roughly corresponds to the maximum of a bright fringe for that pixel. The average fringe separation, Δ, is calculated by averaging the separations of the two minima for all 6000 pixels. The baseline scan is repeated four times, and the baseline data from each pixel for the four scans are averaged to give a final baseline datum for that pixel. The average distance, Δ, between two "dark fringes" is also calculated.

The boundary sharpening is very important step for a successful experiment because assures a good preparation of the initial conditions from which the diffusion process will be investigated in its evolution. The two solutions, the top (less dense) and bottom (more dense), with different composition had to be put in contact in the diffusion channel by moving the crude boundary between them towards the optic axis (the center of the cell). The sharp boundary is obtained drawing the top and bottom solutions out of the cell through the needle with a peristaltic pump (Fig. 4). The sharpening process lasts 30 minutes (for gradient of the salt) and 120 minutes (for gradient of the protein), and typically uses about 75 ml of total fluid.

The fractional part of a fringe (fpf) is obtained after the diffusion process begins and the pattern is scanned several times. In a full scan, there are 49 scan increments of 10 μm each giving 50 positions and a span of 490 μm. After each full scan the array is returned to the same starting position. The first 2000 pixels (corresponding to the still uniform bottom solution refractive index) and the last 2000 pixels (corresponding to the uniform top solution refractive index) for the "dark fringe" positions are recorded. The two set of data are first adjusted by baseline corrections and then averaged. We received two average position values corresponding to the refractive index of the bottom and the top solutions. The difference δ between the two average positions is then divided by the fringe separation, Δ, to produce the fpf value.

Diffusion Scans start after the needle is removed and the diffusion patterns can be resolved by the optical scanner. The initial time required before taking the first scan depends on the optical aberrations. Consideration of third order aberrations indicates that we should wait until $t \geq 4.8\times10^{-6} aJ^{3/2}/D_A$ (pseudo-binary diffusion coefficient which could be determined experimentally) for starting the first scan. The last Rayleigh scan should be taken at about 3.5 times the initial time to avoid failure of the free-diffusion boundary conditions. Usually 50 diffusion scans, equally distributed between initial time and final time, are performed following the same procedure like for fpf scans. In Fig. 5 are illustrated three different kind of scans.

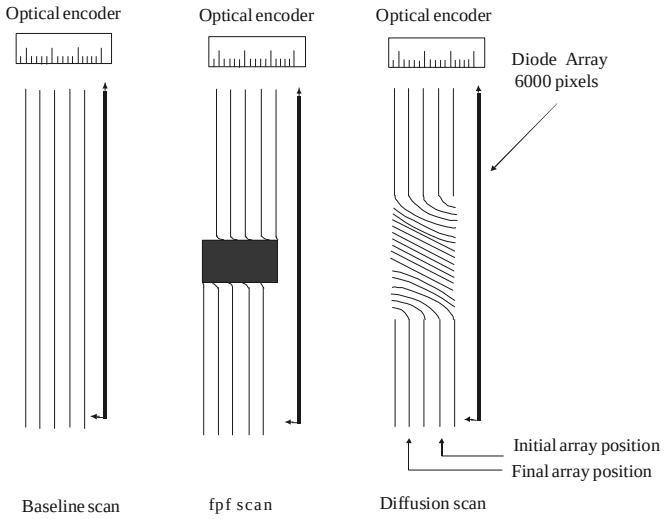

Fig. 5. Geometric set up for the baseline scan, fpf scan and diffusion scan.

Data analysis. The Rayleigh pattern gives the refractive index profile (Fig. 2) along the vertical Z direction. Y "dark fringe" positions for all the 6000 pixels are obtained and converted to the corresponding j values in the following way. If we set $Y = 0$ for the position corresponding to the refractive index of the bottom solution, the j value for an assigned z_j position (identified by one of the 6000 pixels) is given by:

$$j = \frac{Y}{\Delta} + k \tag{29}$$

where k is the number of "dark fringes" crossing the $Y = 0$ line between the starting position and z_j. The total number of fringes J, is given by the total number of intersections occurring on the $Y = 0$ line plus the fpf value. The $f(j)$ values are then calculated and reported as a function of the normalized quantity z_j. The Creeth's pairing method was then applied for 200 equidistant $f(j)$ values, distributed between -1 and +1, to get 100 corresponding average positions $\bar{z}_j$:

$$\bar{z}_j = \frac{1}{2}\left| z_j - z_{J-j} \right| \tag{30}$$

The $f(j)$ values, reported as a function of $\bar{z}_j$, with j ranging between $J/2$ and J, are then analyzed to produce 100 "local" diffusion coefficients, D_j, defined by:

$$f(j) = erf\left(\bar{z}_j / \sqrt{D_j}\right) \qquad \text{where} \qquad D_j = \left[\frac{\bar{z}_j}{erfinv[f(j)]}\right]^2 \tag{31}$$

Due to the nature of the refractive index profile, only the D_j values obtained within $0.30 \le f(j) \le 0.86$ are considered accurate and used for further analysis.

Also, due to the imperfection of the initial solution interface, it is impossible to have a good

estimate for the time elapsed between a perfect initial condition and the diffusion scan (the error is a measure of the initial boundary quality). The true time, t, values could be obtained by taking several diffusion scans and recording the clock time, t'. The error $\Delta t = t - t'$ caused by underestimation of t, is directly related to the incorrect estimation of $D_j^{'}$ and D_j by:

$$D_j \cdot t = D_j' \cdot t' \tag{32}$$

This relation is true also for the averaged values $\overline{D}$ and $\overline{D}'$, without losing generality:

$$\overline{D}' = \overline{D}\left(1 + \frac{\Delta t}{t'}\right) \tag{33}$$

and a linear least square of $\overline{D}'$ versus $1/t'$ yields $\overline{D}$ and Δt. The multicomponent systems, after Δt correction, are analyzed with the methods reported in the theoretical approach.

For a multicomponent system, the number of experiments necessary to be performed at certain appropriate experimental refractive fraction, α, is directly related to the corresponding number of diffusion coefficients necessary for transport characterization. For statistical reasons we performed four experiments in the ternary case. The choice of α values is also regulated by statistical needs. In the ternary case experiment, orthogonality was considered as a criteria for statistics optimization. We used the following values for α: two experiments were performed at $\alpha = 0$ and the other two at $\alpha = 1$ [19, 20]. Changes in the chosen α's are related to the system limitations such as gravitational instability or thermodynamic instability (lysozyme precipitation).

The experimental results for ternary lysozyme-Na_2SO_4-water diffusion coefficients are given below in the Tables 1,2,3 for a mean concentration 0.6 mM for lysozyme and 0.1, 0.25, 0.5, 0.65 and 0.8 M for Na_2SO_4 at T=298 K and pH = 4.5. The subscript v denotes the volume-fixed frame of reference:

Table 1. The four diffusion coefficients for ternary lyzsozyme-Na_2SO_4-water for C_1 = 0.6 mM and C_2 = 0.1 M and 0.25 M.

Diffusion coefficients	C_1 = 0.6000 C_2 = 0.1000	C_1 = 0.6000 C_2 = 0.2500
$(D_{11})_v (10^{-9} m^2 s^{-1})$	0.1169± 0.0001	0.1090± 0.0001
$(D_{12})_v (10^{-9} m^2 s^{-1})$	- 0.000013± 0.000001	0.000108± 0.000001
$(D_{21})_v (10^{-9} m^2 s^{-1})$	2.49± 0.01	4.14± 0.01
$(D_{22})_v (10^{-9} m^2 s^{-1})$	0.9661± 0.0001	0.8826± 0.0001

Table 2. The four diffusion coefficients for ternary lyzsozyme-Na_2SO_4-water for C_1 = 0.6 mM and C_2 = 0.5 M and 0.65 M.

Diffusion coefficients	C_1 = 0.6000 C_1 = 0.5000	0.6000 0.6500
$(D_{11})_v (10^{-9} m^2 s^{-1})$	0.0969± 0.0001	0.0894± 0.0001
$(D_{12})_v (10^{-9} m^2 s^{-1})$	0.000132± 0.000001	0.000134± 0.000001
$(D_{21})_v (10^{-9} m^2 s^{-1})$	6.75± 0.01	8.26 ± 0.01
$(D_{22})_v (10^{-9} m^2 s^{-1})$	0.7791 ± 0.0001	0.7294 ± 0.0001

Table 3. The four diffusion coefficients for ternary lyzsozyme-Na_2SO_4-water for C_1 = 0.6 mM and C_2 = 0.8 M.

Diffusion coefficients	C_1 = 0.6000 C_1 = 0.8000
$(D_{11})_v(10^{-9} m^2 s^{-1})$	0.0822 ± 0.0001
$(D_{12})_v(10^{-9} m^2 s^{-1})$	0.000130 ± 0.000001
$(D_{21})_v(10^{-9} m^2 s^{-1})$	9.50 ± 0.01
$(D_{22})_v(10^{-9} m^2 s^{-1})$	0.6900 ± 0.0001

The values for main-term $(D_{11})_v$ are 13% smaller than the values for the same coefficient but using the lys-NaCl-water ternary system, at the same concentration [21]. The cross-term $(D_{21})_v$ for the flux of Na_2SO_4 caused by the gradient of lysozyme chloride increases as the Na_2SO_4 concentration increases. The values for $(D_{21})_v$ are 25% smaller than the values for the same coefficient using the NaCl as salt [21]. At 0.8 M Na_2SO_4, this term becomes 14 times larger than the Na_2SO_4 main-term diffusion coefficient $(D_{22})_v$. The cross-term $(D_{12})_v$ for the flux of lysozyme caused by the gradient of Na_2SO_4 is small in comparison with all the other diffusion coefficients as it was expected, and 35% smaller than $(D_{12})_v$ in the case of lys-NaCl-water [21]. The ternary main-term $(D_{22})_v$, for the flux of Na_2SO_4 caused by the own gradient of concentration, is 40 % smaller than the $(D_{22})_v$ for ternary lys-NaCl-water [21], for the same range of concentration.

Details on the experimental preparation of solutios and results for densities measurements, partial molar volumes $\overline{V_1}$, $\overline{V_2}$ and $\overline{V_o}$ values for lysozyme, Na_2SO_4 and water respectively, and viscosities values for the ternary lysozyme-Na_2SO_2–Water system, in the same concentration conditions at T = 298 K and pH = 4.5, using the Gosting diffusiometer operating in Rayleigh mode, are given in the work [22].

4. Conclusions

We presented a brief description of the Gosting diffusiometer located in Texas Christian University, an unique instrument with a very good quality for optical and mechanical components. We used this diffusiometer, operating in a Rayleigh interferometric mode, to determine the main-term diffusion coefficients and the cross-term diffusion coefficients for lysozyme-Na_2SO_2-Water, for the first time, by our knowledge. All obtained values for diffusion coefficients were compared with the values for ternary lysozyme-NaCl-water system [21], also for first time presented, from the same Gosting diffusiometer and in the same conditions. In order to determine these coefficients we had to make an experimental analysis work for our system, including five parts: the baseline scans, boundary sharpening, fractional part of fringe scans, diffusion scans and data analysis. All these experimental analyses, for our ternary system, were detailed in this paper.

Acknowledgement

One of the authors (DB) is very grateful to O. Annunziata and J. G. Albright for constant and helpful advice during the experimental work. This research was supported by the Texas Christian University Grant RCAF-11950, by the NASA Microgravity Biotechnology Program through the Grant NAG8-1356, and by the CERES project C4- 164/2004.

References

[1] L. Onsager, Ann. N. Y. Acad. Sci. **46**, 241 (1945)
[2] L. J. Gosting, Advances in Protein Chemistry, M. L. Anson, K. Bailey, J. T. Edsall, Eds.; Academic Press: New York, N. Y., Vol. XI, p 429 (1956)
[3] S. Miyashita, H. Komatsu, Y. Suzuki, T. J. Nakada, Cryst. Growth **141**, 419 (1994)
[4] K. Kurihara, S. Miyashita, G. Sazaki, T. Nakada, Y. Suzuki, H. Komatsu, J. Cryst. Growth **166**, 904 (1996)
[5] F. J. Rosenberger, Cryst. Growth **76**, 618 (1956)
[6] P. G. Vekilov, L. A. Monaco, B. R. Thomas, V. Stojanoff, F. Rosenberger, Acta Crystallogr., Sect D **52**, 785 (1996)
[7] H. Lin, F. Rosenberger, J. I. D. Alexander, A. Nadarajah, J. Cryst. Growth **151**, 153 (1995).
[8] J. Philpot, G. H. Cook, Research **1**, 234 (1948)
[9] D. G. Miller, J. G. Albright, Measurement of the transport Properties of Fluids: Experimental Thermodynamics, W.A. Wakeham, A. Nagashima, J. V. Sengers, Eds., Blackwell Scientific Publications, Oxford, p 272 (1991)
[10] L. J. Gosting, H. Fujita, Abstracts Database, J. Am. Chem. Soc. **79**, 1359 (1957)
[11] H. Fujita, L. J. Gostring, J. Am. Chem. Soc. **78**, 1099 (1956)
[12] J. M. Creeth, J. Am. Chem. Soc. **77**, 6428 (1955)
[13] J. M. Creeth, L. J. Gosting, J. Phys. Chem., **62**, 58 (1958)
[14] J. M. Creeth, J. Phys. Chem., **62**, 66 (1958)
[15] D. G. Miller, J. Phys. Chem., **92**, 4222 (1988)
[16] L. J. Gosting, L. H. Kim, M. A. Loewenstein, G. Reifelds, A. Revzin, Rev. Sci. Instrum. **44**, 1602 (1973)
[17] M. E. Zeidler, J. G. Albright, D. G. Miller, Rev. Sci. Instrum. (submitted).
[18] D. G. Miller, J. G. Albright, R. Mathew, C. M. Lee, J. A. Rard, L. B. Eppstein, J. Phys. Chem. **97**, 3885 (1993)
[19] J. A. Rard, J. G. Albright, D. G. Miller, M. E, Zeidler, J. Chem. Soc. Faraday Trans. **92**, 4187 (1996)
[20] M. C. Yang, J. G. Albright, J. A. Rard, D. G. Miller, J. Solution Chem. **27**, 309 (1998)
[21] J. G. Albright, O. Annunziata, D. G. Miller, L. Paduano, A. J. Pearlstein, J. Am. Chem. Soc. **121**, 3256-3266 (1999)
[22] D. Buzatu, E. Petrescu, C. Popa, F. D. Buzatu, J. G. Albright, Rev. Chim. **55**(6), 435 (2004)